

Closed-Loop Wireless Power Transfer with Adaptive Waveform and Beamforming: Design, Prototype, and Experiment

Shanpu Shen, *Member, IEEE*, Junghoon Kim, *Member, IEEE*, and Bruno Clerckx, *Senior Member, IEEE*

Abstract—In this paper, we design, prototype, and experiment a closed-loop radiative wireless power transfer (WPT) system with adaptive waveform and beamforming using limited feedback. Spatial and frequency domains are exploited by jointly utilizing multi-sine waveform and multi-antenna beamforming at the transmitter in WPT system to adapt to the multipath fading channel and boost the output dc power. A closed-loop architecture based on a codebook design and a low complexity over-the-air limited feedback using an IEEE 802.15.4 RF interface is proposed. The codebook consists of multiple codewords where each codeword represents particular waveform and beamforming. The transmitter sweeps through the codebook and then the receiver feeds back the index of the optimal codeword, so that the waveform and beamforming can be adapted to the multipath fading channel to maximize the output dc power without requiring explicit channel estimation and the knowledge of accurate Channel State Information. The proposed closed-loop WPT with adaptive waveform and beamforming using limited feedback is prototyped using a Software Defined Radio equipment and measured in a real indoor environment. The measurement results show that the proposed closed-loop WPT with adaptive waveform and beamforming can increase the output dc power by up to 14.7 dB compared with the conventional single-tone and single-antenna WPT system.

Index Terms—Beamforming, closed-loop, limited feedback, multi-sine, multiple antennas, waveform, wireless power transfer.

I. INTRODUCTION

WIRELESS power transfer (WPT) via radio-frequency (RF) has gained increasing interests as a promising technology to energize a large number of low-power and low duty-cycle devices in applications such as the Wireless Sensor Networks and Internet of Things [1]. WPT utilizes a dedicated transmitter to radiate RF energy through a wireless channel and a rectifying antenna (rectenna) to receive and convert the RF energy into dc power. Compared with batteries which required to be replaced and recharged periodically, WPT is more reliable, controllable, user-friendly, and cost-effective.

However, a crucial challenge of radiative WPT is to increase the output dc power of the rectenna given a fixed transmit power, or equivalently to enhance end-to-end power transfer efficiency. To that end, the vast majority of the research has

focused on designing efficient rectenna to increase the output dc power. Various techniques to enhance the rectenna design include using multiband rectenna [2]-[5], multiport rectenna [6]-[10], compact rectenna [11], [12], metasurface rectenna [13], [14], tightly coupled array rectenna [15], [16], multiband and broadband rectifier [17], [18], high-efficiency rectifier [19]-[22], reconfigurable rectifier [23], and hybrid RF-solar harvester [24], [25].

Another and complementary research area to increase the output dc power is to design efficient WPT signals [26], [27]. One promising signal strategy is the waveform. Efficient waveforms can indeed increase the output dc power in WPT. Due to the nonlinearity of rectifier, the RF-to-dc efficiency depends on not only the input RF power level but also the waveform shape [28]. It has been shown through simulations and experiments that the RF-to-dc efficiency can be improved by waveforms with high peak to average power ratio (PAPR), such as multi-sine waveforms [29]-[32] and other waveforms including orthogonal frequency division multiplexing (OFDM), white noise, chaotic [33]. However, there are two limitations in these works [29]-[33]. *First*, they ignore the multipath fading in the wireless channel between the transmitter and the receiver, though multipath makes the waveform input into the rectifier at the receiver different from the waveform transmitted by the transmitter. *Second*, they are based on an open-loop system with the waveform being static and designed without considering any Channel State Information (CSI) of multipath fading channel, which degrades the output dc power. Therefore, a closed-loop WPT system with waveform adaptive to the multipath fading channel is needed [34].

Using multiple antennas at the transmitter with efficient beamforming is another effective signal strategy to increase the output dc power in WPT. By using beamforming, the RF signal transmitted by each antenna element can be coherently added together at the receiver so as to increase the output dc power [35]. Various WPT systems with beamforming have been prototyped including using digital beamforming through baseband precoding [36], analog beamforming through phased array [37], and time-modulation array [38], [39]. Particularly, a selective and tracking WPT system using backscattering for feedback has been designed in [36] and WPT systems with adaptive beamforming using receive signal strength indicator feedback have been designed in [40]-[42]. In addition, WPT systems with adaptive beamforming using the second and third harmonics for feedback have been designed in [43]-[45]. However, the limitation of these works [36]-[45] is that

Manuscript received; This work was supported in part by the EPSRC of U.K. under Grant EP/P003885/1 and EP/R511547/1. (*Corresponding author: Shanpu Shen.*)

The authors are with the Department of Electrical and Electronic Engineering, Imperial College London, London SW7 2AZ, U.K. (e-mail: s.shen@imperial.ac.uk; junghoon.kim15@imperial.ac.uk; b.clerckx@imperial.ac.uk).

they only focus on using beamforming but did not consider using efficient waveform design. Therefore, together with the two aforementioned limitations of the WPT waveform designs [29]-[33], it is found that a closed-loop WPT system with both waveform and beamforming adaptive to the multipath fading channel is needed.

A unified and systematic theoretical design of closed-loop WPT system with adaptive waveform and beamforming was first conducted in [46], with further notable extensions in [47]-[50]. Simulations in those papers demonstrated the significant benefits of a systematic design of adaptive waveform and beamforming. However, results were not demonstrated experimentally. In [51], and more recently in [52], the first experimental WPT system with adaptive waveform and beamforming was prototyped and experimented, and results demonstrated the significant benefits in terms of dc power and range expansion of a WPT architecture relying on channel-adaptive waveform and beamforming. However, those experimental works used complex channel estimation at the receivers (based on OFDM channel estimation and pilot transmission, reminiscent of communication system) and cable feedback mechanisms that do not lend themselves easily to real-world setup with energy-constrained devices. The limitation of those experimental works is therefore that they did not address the challenging problem of energy-efficient and low complexity CSI acquisition at the transmitter. In addition, a WPT system with distributed antennas using channel-adaptive antenna selection and frequency selection has been designed, prototyped, and experimented in [53]. However, antenna selection is less efficient compared to beamforming and frequency selection is less efficient compared to multi-sine waveform, which limit the output dc power.

In this paper, we design, prototype, and experimentally validate the first closed-loop WPT system with adaptive waveform and beamforming using over-the-air limited feedback technique to increase the output dc power. The contributions of the paper are summarized as follows.

First, we propose a closed-loop WPT architecture that exploits frequency and spatial domains and the nonlinearity of rectifier by jointly utilizing multi-sine waveform and multi-antenna beamforming at the transmitter to effectively increase the output dc power. The architecture uniquely relies on a codebook design and a low complexity over-the-air limited feedback using an IEEE 802.15.4 RF interface. The codebook is predefined and consists of multiple codewords where each codeword represents particular waveform and beamforming. During a training phase, the transmitter sweeps through the codebook and the receiver measures the output dc power for each codeword and feeds back the index of the optimal codeword to the transmitter. Then, the transmitter can transfer power using the optimal waveform and beamforming during a WPT phase. The operation is repeated periodically. With the designed codebook and limited feedback, the channel estimation and accurate CSI can be avoided and more importantly the multi-sine waveform and multi-antenna beamforming at the transmitter can be optimized to adapt to the multipath fading channel in real time.

Second, we devise, prototype, and experimentally verify the

proposed closed-loop WPT system with adaptive waveform and beamforming using limited feedback by leveraging a Software Defined Radio (SDR) equipment. To the authors' best knowledge, it is the first prototype of a closed-loop WPT system with adaptive waveform and beamforming using over-the-air limited feedback. We measure the proposed WPT system prototype in a real indoor environment. A closed-loop WPT system based on cable-feedback and an open-loop WPT system are also measured as comparison benchmarks. The measurement results show that using closed-loop adaptive multi-sine waveform and multi-antenna beamforming can effectively increase the output dc power. Compared with the conventional 1-tone 1-antenna WPT system, the proposed closed-loop WPT system with adaptive waveform and beamforming can increase the output dc power by up to 14.7 dB. In addition, compared with the cable-feedback based closed-loop WPT system, the proposed closed-loop WPT system using limited feedback can achieve similar performance while it is more practical since it does not require knowing the CSI.

Organization: Section II describes a closed-loop WPT system model with limited feedback. Section III provides the closed-loop WPT system design with adaptive waveform and beamforming. Section IV provides the experimental setup and measurement results. Section V concludes the work.

Notations: Bold lower letters stands for vectors. A symbol not in bold font represents a scalar. $\Re\{x\}$ and $|x|$ refer to the real part and modulus of a complex scalar x , respectively. $\|\mathbf{x}\|$, \mathbf{x}^T , and \mathbf{x}^H refer to the l_2 -norm, transpose, and conjugate transpose of a vector \mathbf{x} , respectively.

II. CLOSED-LOOP WIRELESS POWER TRANSFER

A. System Model

We consider a multi-sine multi-antenna WPT system. There are M antennas at the transmitter and one antenna at the receiver. A multi-sine waveform consisting of N tones at angular frequencies $\omega_1, \omega_2, \dots, \omega_N$ is transmitted. The multi-sine waveform transmitted by the m th transmit antenna is given by

$$x_m(t) = \Re \left\{ \sum_{n=1}^N s_{m,n} e^{j\omega_n t} \right\}, \quad (1)$$

where $s_{m,n}$ is a complex weight accounting for the magnitude and phase of the n th tone on the m th transmit antenna. We group $s_{m,n}$ into a vector $\mathbf{s}_n = [s_{1,n}, s_{2,n}, \dots, s_{M,n}]^T$ which characterizes the beamforming at the n th tone. Furthermore, we group $\mathbf{s}_n \forall n$ into a vector $\mathbf{s} = [\mathbf{s}_1^T, \mathbf{s}_2^T, \dots, \mathbf{s}_N^T]^T$ which characterizes the waveform and beamforming. The transmitter is subject to a transmit power constraint given by

$$\frac{1}{2} \|\mathbf{s}\|^2 \leq P, \quad (2)$$

where P denotes the transmit power.

The multi-sine waveform transmitted by the multiple transmit antennas propagate through a wireless channel. The waveform received by the receiver can be expressed as

$$y(t) = \Re \left\{ \sum_{n=1}^N \mathbf{h}_n \mathbf{s}_n e^{j\omega_n t} \right\}, \quad (3)$$

where $\mathbf{h}_n = [h_{1,n}, h_{2,n}, \dots, h_{M,n}]$ with $h_{m,n}$ referring to the complex channel gain between the m th transmit antenna and the receive antenna at the n th angular frequency. Due to the multipath fading channel, the received waveform $y(t)$ is different from the transmitted waveform $x_m(t)$. Therefore, we need to consider the multipath fading channel when designing the optimal waveform and beamforming for WPT. From (3), the received RF power is given by

$$P_{\text{RF}} = \frac{1}{2} \sum_{n=1}^N |\mathbf{h}_n \mathbf{s}_n|^2. \quad (4)$$

The received waveform is input into a rectifier to generate output dc power. The output dc power is denoted as P_{DC} and given by

$$P_{\text{DC}} = P_{\text{RF}} \eta(y(t)) = P_{\text{DC}}(\mathbf{h}_1, \mathbf{h}_2, \dots, \mathbf{h}_N, \mathbf{s}), \quad (5)$$

where $\eta(y(t))$ refers to the RF-to-dc efficiency with the input waveform $y(t)$. From (3) and (4), the output dc power is a function of the wireless channel gains $\mathbf{h}_n \forall n$ and the waveform and beamforming weight vector \mathbf{s} , denoted as $P_{\text{DC}}(\mathbf{h}_1, \mathbf{h}_2, \dots, \mathbf{h}_N, \mathbf{s})$.

Assuming the CSI, i.e. the wireless channel gains $\mathbf{h}_n \forall n$, is known at the transmitter, the waveform and beamforming weight vector \mathbf{s} can be optimized to adapt to the channel to maximize the output dc power, which can be formulated as

$$\max_{\mathbf{s}} P_{\text{DC}}(\mathbf{h}_1, \mathbf{h}_2, \dots, \mathbf{h}_N, \mathbf{s}) \quad (6)$$

$$\text{s.t.} \quad \frac{1}{2} \|\mathbf{s}\|^2 \leq P. \quad (7)$$

In the next subsections, we provide two strategies for designing adaptive waveform and beamforming to maximize the output dc power.

B. Scaled Matched Filter

Scaled Matched Filter (SMF) is a low complexity strategy to optimize the waveform and beamforming [48]. Using SMF, the beamforming weight vector \mathbf{s}_n can be expressed as

$$\mathbf{s}_n = c \|\mathbf{h}_n\|^\beta \frac{\mathbf{h}_n^H}{\|\mathbf{h}_n\|}, \quad \forall n, \quad (8)$$

where $\beta \geq 1$ is a parameter controlling the magnitude (l_2 -norm) of \mathbf{s}_n and c is a constant satisfying the transmit power constraint and is given by

$$c = \sqrt{\frac{2P}{\sum_{n=1}^N \|\mathbf{h}_n\|^{2\beta}}}. \quad (9)$$

The SMF waveform and beamforming design is only a function of the single parameter β . We set $\beta = 3$ in this work. In [48], it has been shown through simulation that the performance of SMF strategy with $\beta = 3$ is close to that of the optimal waveform and beamforming design proposed in [46] but at a much lower computational complexity.

Although the SMF has good performance and low computational complexity, it requires that the transmitter has the knowledge of CSI, i.e. $\mathbf{h}_n \forall n$. Acquiring the CSI at the transmitter is challenging in WPT since it needs channel

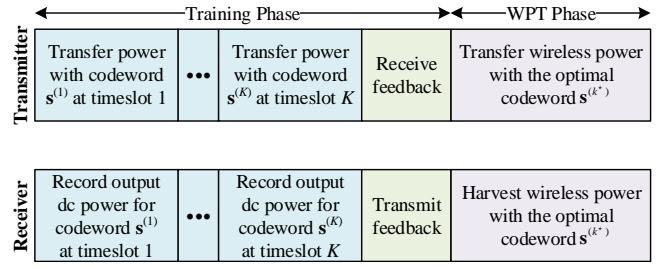


Fig. 1. Time frame for the closed-loop WPT using limited feedback strategy.

estimation which increases the power consumption and circuit complexity. To overcome this challenge, in the next subsection, we provide another waveform and beamforming design strategy based on limited feedback.

C. Limited Feedback

Consider a codebook consisting of K codewords, denoted as $\mathbf{s}^{(1)}, \mathbf{s}^{(2)}, \dots, \mathbf{s}^{(K)}$, with each codeword representing a particular waveform and beamforming weight vector. The basic idea of limited feedback strategy is to select the optimal codeword in the codebook to maximize the output dc power. Specifically, the transmitter and receiver cooperatively work frame by frame and the frame period is designed to be smaller than the coherence time of the channel such that the wireless channel gains $\mathbf{h}_n \forall n$ are constant during one frame. As shown in Fig. 1, each frame has two phases: training phase and WPT phase. The training phase is to find the optimal codeword, i.e. the optimal waveform and beamforming, while the WPT phase is to transfer the wireless power with the optimal waveform and beamforming. During the training phase, the transmitter sequentially chooses the K codewords as its waveform and beamforming to transfer wireless power while in the meantime the receiver will record the output dc power for each codeword. The output dc power for the k th codeword $\mathbf{s}^{(k)}$ is given by $P_{\text{DC}}(\mathbf{h}_1, \mathbf{h}_2, \dots, \mathbf{h}_N, \mathbf{s}^{(k)})$. After recording the output dc power for all the codewords, the receiver can find the index of the optimal codeword maximizing the output dc power as

$$k^* = \underset{k=1, \dots, K}{\operatorname{argmax}} P_{\text{DC}}(\mathbf{h}_1, \mathbf{h}_2, \dots, \mathbf{h}_N, \mathbf{s}^{(k)}). \quad (10)$$

Then, the receiver feeds back the index of the optimal codeword k^* to the transmitter. Since there are K codewords in the codebook, we only need to feed back $\lceil \log_2 K \rceil$ bits representing the index of the optimal codeword, where $\lceil \cdot \rceil$ refers to the ceiling function. Once the transmitter receives the feedback k^* , it can use the optimal codeword $\mathbf{s}^{(k^*)}$ as its waveform and beamforming to efficiently transfer wireless power during the WPT phase.

In contrast with the SMF strategy, the limited feedback strategy can adapt to the wireless channel to increase the output dc power without requiring the knowledge of CSI, i.e. $\mathbf{h}_n \forall n$. Due to such benefit, we focus on using the limited feedback strategy to implement our closed-loop WPT system in this work. The key of limited feedback strategy in WPT is the design of an efficient codebook, which should have diverse codewords to match different wireless channel gains.

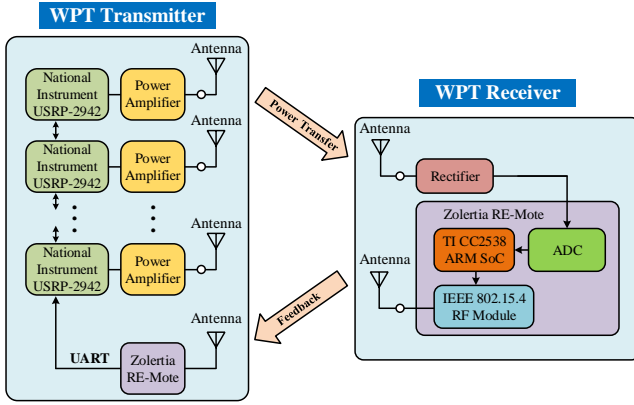


Fig. 2. Schematic diagram of the closed-loop WPT system with adaptive waveform and beamforming using limited feedback.

In this work, we design an efficient codebook by following the approach proposed in [49]. Such approach leverages the statistics of the multipath fading channel and the rectifier nonlinearity and simulation results have shown that it can provide high output dc power. In addition, increasing the codebook size K is beneficial to increase the output dc power as there are more codewords to select, however, at the expense of feeding back more bits.

In the next section, we provide a design for the closed-loop WPT system with adaptive waveform and beamforming using limited feedback.

III. CLOSED-LOOP WPT SYSTEM DESIGN

The schematic diagram of the proposed closed-loop WPT system with adaptive waveform and beamforming using limited feedback is shown in Fig. 2. In the following subsections, we separately describe the designs for transmitter, receiver, and flow chart of the closed-loop WPT system.

A. Transmitter Design

The transmitter consists of two parts. The first part is made up by multiple antennas, power amplifiers, and SDR equipment, which is used to generate and radiate RF signals with waveform and beamforming characterized by different codewords. There are M transmit antennas in the first part and we consider three cases with $M = 1, 2,$ and 4 . All the antennas are identical 2.4-GHz monopole antennas which have omnidirectional radiation patterns with 3 dBi antenna gain and 85% radiation efficiency. Each antenna is connected to a power amplifier, Mini-Circuits ZHL-16W-43-S+, which has a gain of 45 dB and amplifies the RF signal generated by SDR equipment, and the total transmit power is set to 33 dBm (2W). The SDR equipment, National Instrument (NI) USRP-2942, can generate multi-sine waveforms with different magnitudes and phases at each tone. The multi-sine waveform has N tones and we consider four cases with $N = 1, 2, 4,$ and 8 . The N tones are centered around 2.4 GHz with a uniform frequency gap $\Delta_f = B/N$ where the bandwidth $B = 10$ MHz. We use multiple USRP-2942 to generate multi-sine waveform for each

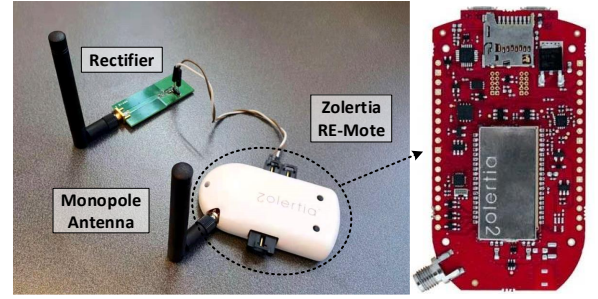


Fig. 3. Photo of the receiver in the proposed closed-loop WPT system and the Zolertia RE-Mote.

transmit antenna so as to implement the multi-sine waveform and multi-antenna beamforming.

The second part is made up by a 2.4-GHz monopole antenna and a Zolertia RE-Mote, which is used to communicate with the receiver and acquire the optimal codeword fed back from the receiver. The Zolertia RE-Mote is a hardware development platform consisting of the Texas Instruments CC2538 ARM Cortex-M3 system on chip (SoC) and an on-board 2.4 GHz IEEE 802.15.4 RF interface. The photo of the Zolertia RE-Mote is shown in Fig. 3. In the Zolertia RE-Mote, we use a Contiki operating system as a software platform. The Zolertia RE-Mote at the transmitter is used to communicate with the receiver, which is also equipped with a Zolertia RE-Mote, through the built-in IEEE 802.15.4 RF interface operating at 2.42 GHz (that is different from the frequency of the multi-sine waveform for WPT). Specifically, the Zolertia RE-Mote at the transmitter sends a message to the receiver to start the program and it also receives the index of the optimal codeword fed back from the receiver, so that the transmitter can transfer the wireless power with the optimal waveform and beamforming to maximize the output dc power.

B. Receiver Design

The receiver consists of two parts as shown in Fig. 3. The first part is a rectenna that receives RF signal and converts it to dc power. It consists of a single diode rectifier and 2.4-GHz monopole antenna with 3 dBi gain and 85% radiation efficiency. We reuse the single diode rectifier design in [53] for simplicity because this work focuses on designing a closed-loop WPT system with adaptive waveform and beamforming instead of focusing on rectifier design. The topology and measured RF-to-dc efficiency of the single diode rectifier are shown in Fig. 4. The rectifier consists of an impedance matching network, a single rectifying diode, a low pass filter, and a load. The Schottky diode Skyworks SMS7630 is chosen as the rectifying diode as it has a low turn-on voltage, which is suitable for low power rectifier. Common materials including the 1.6-mm-thick FR-4 substrate and lumped elements are used to simplify the rectifier fabrication. The values of the elements in the matching network and low pass filter are optimized to maximize RF-to-dc efficiency at low input RF power.

The second part is made up by a 2.4-GHz monopole antenna and a Zolertia RE-Mote, which is used to record the output dc voltage of the rectenna, communicate with the transmitter, and

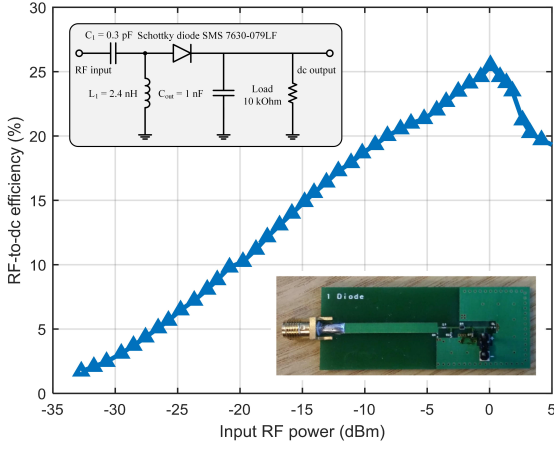


Fig. 4. Topology of the single diode rectifier and its measured RF-to-dc efficiency.

feed back the index of the optimal codeword to the transmitter. The Zolertia RE-Mote at the receiver receives the message from the transmitter to start the program and then it records the output dc voltage of the rectenna through a built-in analog-to-digital converter (ADC). The recorded output dc voltages are processed by the CC2538 ARM Cortex-M3 SoC in the Zolertia RE-Mote and the index of the optimal codeword is found and fed back to the transmitter through the built-in IEEE 802.15.4 RF interface so that the transmitter can transfer the wireless power with the optimal waveform and beamforming.

C. Flow Chart

The flow chart of the adaptive closed-loop WPT system with adaptive waveform and beamforming using limited feedback is shown in Fig. 5. The transmitter and receiver cooperatively work frame by frame. Each frame has two phases: training phase and WPT phase, as shown in Fig. 5. The training phase is to find the optimal codeword, i.e. the optimal waveform and beamforming, while the WPT phase is to transfer the wireless power with the optimal waveform and beamforming.

In the training phase, the Zolertia RE-Mote at the transmitter first sends a message to the receiver through the built-in IEEE 802.15.4 RF interface so that the receiver will start to work. It also sends a message to the NI USRP-2942 through UART so that the NI USRP-2942 will start to work. The NI USRP-2942 sequentially chooses each codeword as its waveform and beamforming to transfer wireless power. The time duration for transferring wireless power for each codeword is $T_s = 10 \text{ ms}$. In the meantime, the receiver will measure and record the corresponding output dc voltage of the rectenna for each codeword through the built-in ADC in Zolertia RE-Mote. After the Zolertia RE-Mote at the receiver records the output dc voltage for all codewords, it finds the optimal codeword that maximizes the output dc voltage. Generally, for a codebook having K codewords, the receiver only needs to feed back $\lceil \log_2 K \rceil$ bits representing the index of the optimal codeword. In this work, we consider codebooks having 2, 4, 8, 16, 32, and 64 codewords so that the receiver only needs to feed back 1, 2, 3, 4, 5, and 6 bits, respectively, to the transmitter through

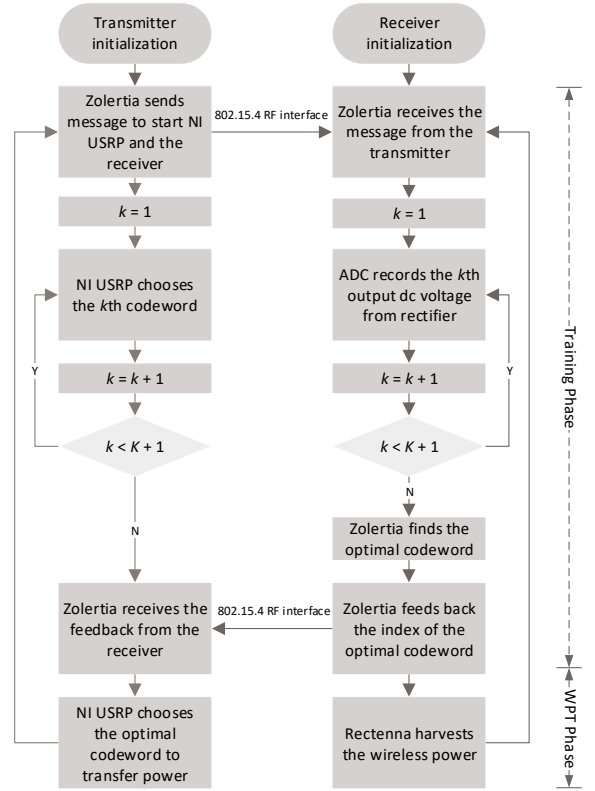


Fig. 5. Flow chart of the closed-loop WPT system with adaptive waveform and beamforming using limited feedback.

the IEEE 802.15.4 RF interface. The Zolertia RE-Mote at the transmitter forwards the received feedback to NI USRP-2942 through UART so that the transmitter can choose the optimal codewords as its waveform and beamforming to transfer wireless power. By this way, we can implement the limited feedback closed-loop WPT system where the waveform and beamforming are adaptive to the wireless fading channel to increase the output dc power without requiring the knowledge of CSI. The time duration for the training phase is KT_s . T_s is dependent on the clock and timer setup in NI USRP-2942, which can be modified by programming. To accelerate the training phase, a smaller T_s can be set in NI USRP-2942, however, T_s cannot be too small since the output dc voltage for a given codeword needs some time to be stable for ADC sampling. If T_s is very small, the output dc voltage is not stable and the dc voltage sampled by ADC is not accurate so that the optimal codeword cannot be found.

In the WPT phase, the transmitter transfers the wireless power with the optimal waveform and beamforming. In the meantime, the receiver harvests the wireless power. When the WPT phase is over, it goes to the next frame and the time duration for one frame is set as $T = KT_s + T_p = 2 \text{ s}$ where T_p denotes the time duration for the WPT phase. In other words, the proposed closed-loop WPT system periodically adapts to the wireless fading channel to maximize the output dc power.

It should be noted that the proposed closed-loop WPT system inherently captures the nonlinearity of rectifier since the selection of the codeword is made at the output dc power

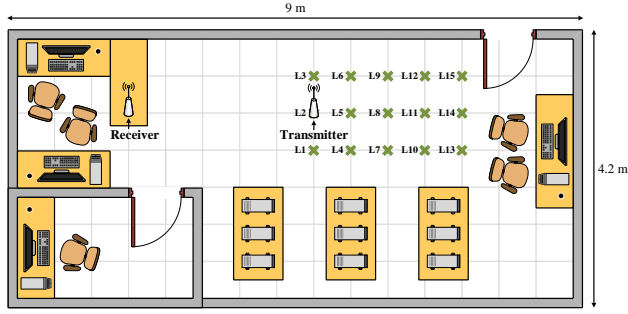


Fig. 6. Illustration of the indoor environment for measurement.

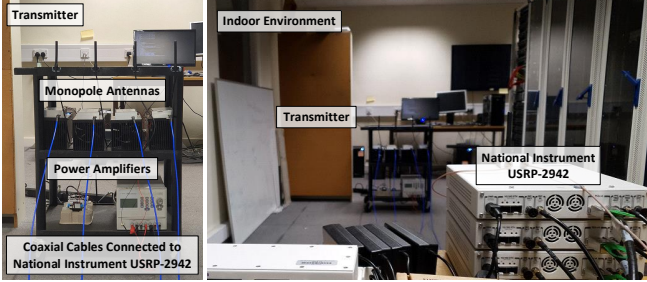


Fig. 7. Photos of the proposed closed-loop WPT system measurement in an indoor environment.

level (instead of RF power), hence capturing the influence of the input signal on the RF-to-dc efficiency.

IV. CLOSED-LOOP WPT SYSTEM EXPERIMENT

To verify the proposed closed-loop WPT system with adaptive waveform and beamforming using limited feedback, we prototype and experiment it in a $4.2\text{m} \times 9\text{m}$ indoor environment. As illustrated in Fig. 6, the indoor environment is equipped with common facilities such as chairs, tables, and computers, so that multipath fading exists in the wireless channel. In Fig. 6, the transmitter is placed at 3 \times 5 different locations marked as L1, L2, ..., and L15 while the receiver is placed at a fixed location, so as to measure the performance of the proposed closed-loop WPT system at different locations. The photos of the proposed closed-loop WPT system measurement in an indoor environment are shown in Fig. 7.

We consider using codebooks having 2, 4, 8, 16, 32, and 64 codewords for the proposed closed-loop WPT system, which correspond to feeding back 1, 2, 3, 4, 5, and 6 bits. In addition, we also consider two benchmarks for comparison. The first benchmark is the SMF, which is a closed-loop strategy as shown in Section II. For the SMF strategy, the receiver performs complex channel estimation by using OFDM channel estimation and pilot transmission as shown in [51] and then feeds back the estimated CSI to the transmitter using cable. Such cable-based feedback is not practical but herein we just use it as a benchmark since it provides almost perfect CSI feedback (equivalently a large number of bits of feedback) to the transmitter. On the other hand, the second benchmark is the uniform power allocation (UP), which is an open-loop strategy allocating the same magnitude and phase to multiple

tones and multiple antennas at the transmitter. Specifically, the complex weights for the UP strategy are given by

$$s_{m,n} = \sqrt{\frac{2P}{MN}}, \forall m, n, \quad (11)$$

which are independent of the CSI. Therefore, the UP strategy can be equivalently viewed as 0 bit of feedback.

A. Adaptive Beamforming Only

First, we show the benefit of closed-loop WPT system with only adaptive beamforming using limited feedback. To that end, we consider the three strategies with only 1 tone and different numbers of transmit antennas, 1, 2, and 4. We use a multimeter to measure the output dc power of the rectifier at locations L1-L15 and average the output dc power over the 15 locations. The average output dc power for the three strategies versus the number of transmit antennas with only 1 tone is shown in Fig. 8. We make the following observations.

1) The average output dc power increases with the number of transmit antennas for the SMF and limited feedback strategies, showing the benefit of multi-antenna adaptive beamforming to increase the output dc power. For the open-loop UP strategies, increasing the number of transmit antenna however reduces the output dc power. It is because the beam of multiple antennas using the UP strategy has fixed direction and narrow beamwidth, which leads to beam misalignment between the transmitter and receiver and reduces the output dc power.

2) The closed-loop SMF and limited feedback strategies achieves higher output dc power than the open-loop strategy UP, showing the benefit of using closed-loop strategies to adapt beamforming to the wireless multipath fading channels.

3) The average output dc power for the limited feedback strategy increases with the number of feedback bits. In other words, using more codewords is beneficial to increase the output dc power. Particularly, when the codebook has enough diverse codewords, the limited feedback strategy can achieve a similar performance to the SMF strategy while having the benefit that it does not require knowing the CSI.

Overall, the measurement results in Fig. 8 show the benefit of closed-loop WPT system with only adaptive beamforming using limited feedback to increase the output dc power.

B. Adaptive Waveform Only

Next, we show the benefit of closed-loop WPT system with only adaptive waveform using limited feedback. To that end, we consider the three strategies with only 1 transmit antenna and different numbers of tones, 1, 2, 4, and 8. We measure the output dc power at locations L1-L15 and average the output dc power over the 15 locations. The average output dc power for the three strategies versus the number of tones with only 1 transmit antenna is shown in Fig. 9. We make the following observations.

1) The average output dc power increases with the number of tones for the three strategies, showing the benefit of using multi-sine waveform in WPT to increase the output dc power.

2) The closed-loop SMF and limited feedback strategies with more than 3 feedback bits achieves higher output dc

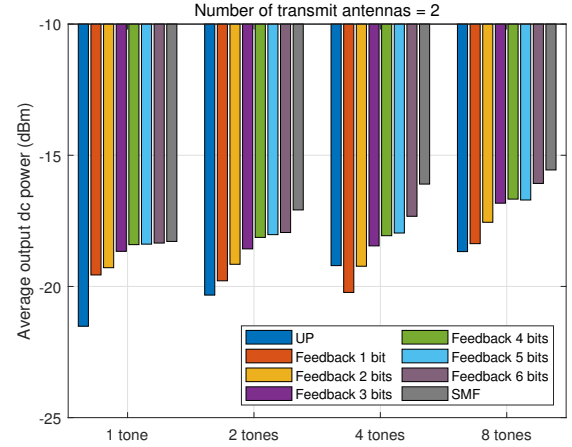
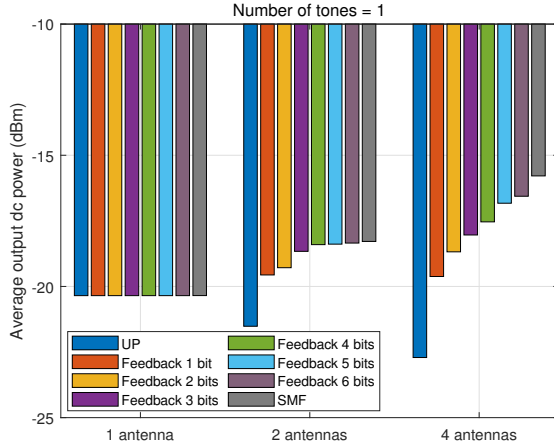


Fig. 8. Average output dc power for the three strategies versus the number of transmit antennas with only 1 tone.

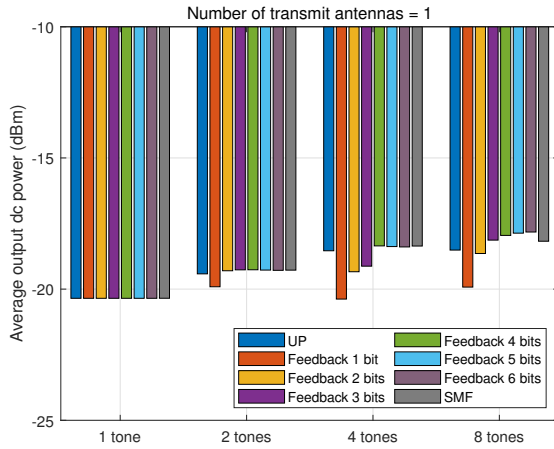


Fig. 9. Average output dc power for the three strategies versus the number of tones with only 1 transmit antenna

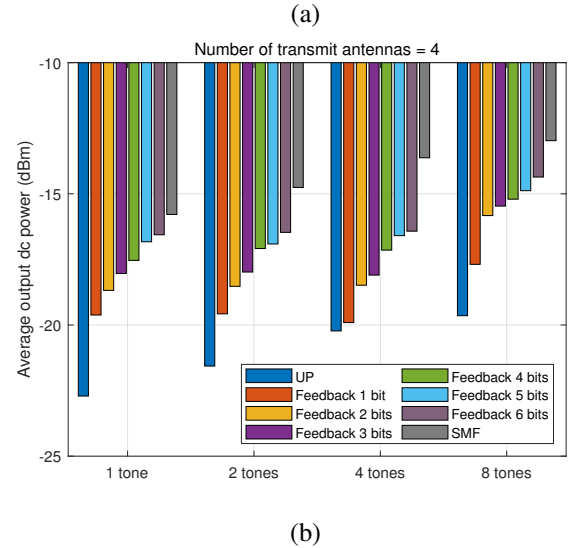


Fig. 10. Average output dc power for the three strategies versus the number of tones with (a) 2 transmit antennas and (b) 4 transmit antennas.

power than the open-loop strategy UP, showing the benefit of using closed-loop strategies to adapt waveform to the wireless multipath fading channels.

3) The average output dc power for the limited feedback strategy increases with the number of feedback bits, or the number of codewords, which is same as the adaptive beamforming only case. When the codebook has enough diverse codewords, the limited feedback strategy has a similar performance to the SMF strategy.

Overall, the measurement results in Fig. 9 show the benefit of closed-loop WPT system with only adaptive waveform using limited feedback to increase the output dc power.

C. Adaptive Waveform and Beamforming

Finally, we show the benefit of closed-loop WPT system with joint adaptive waveform and beamforming using limited feedback. To that end, we consider the three strategies with different numbers of transmit antennas, 2, 4, and different numbers of tones, 1, 2, 4, and 8. We measure the output dc

power at locations L1-L15 and average the output dc power over the 15 locations. The average output dc power for the three strategies versus the number of tones with different numbers of transmit antennas is shown in Fig. 10. We make the following observations.

1) Comparing the 8-tone cases and 1-tone cases in Fig. 10 (a) and (b), we can find that using the joint adaptive waveform and beamforming achieves higher output dc power than using the adaptive beamforming only.

2) Comparing the 1-transmit-antenna case in Fig. 9 and the 2/4-transmit-antenna cases in Fig. 10, we can find that using the joint adaptive waveform and beamforming achieves higher output dc power than using the adaptive waveform only.

3) The closed-loop SMF and limited feedback strategies with more than 1 feedback bit achieves higher output dc power than the open-loop strategy UP, showing the benefit of using closed-loop strategies.

4) The average output dc power for the limited feedback strategy increases with the number of feedback bits, or the number of codewords. When the codebook has enough diverse codewords, the limited feedback strategy has a similar

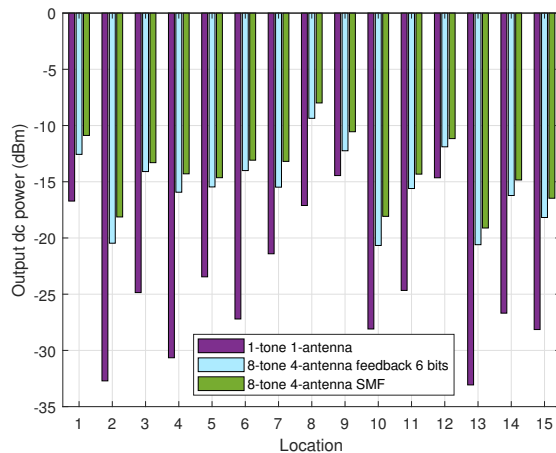


Fig. 11. Output dc power for the 1-tone 1-antenna WPT system, the proposed 8-tone 4-antenna closed-loop WPT system with feeding back 6 bits, and the 8-tone 4-antenna closed-loop WPT system using SMF at different locations.

performance to the SMF strategy.

To further show the benefit of the proposed closed-loop WPT system with adaptive waveform and beamforming, we show the output dc power at different locations for i) the conventional 1-tone 1-antenna WPT system, ii) the proposed 8-tone 4-antenna closed-loop WPT system with feeding back 6 bits, and iii) the benchmark 8-tone 4-antenna closed-loop WPT system using SMF in Fig. 11. Compared with the conventional 1-tone 1-antenna WPT system, using the proposed closed-loop WPT system with adaptive waveform and beamforming can increase the output dc power by 2.2-14.7 dB. In addition, the limited feedback strategy has similar output dc power to the SMF strategy while having the benefit that it does not require knowing the CSI.

Overall, the measurement results in Fig. 10 and Fig. 11 show the benefit of closed-loop WPT system with adaptive waveform and beamforming using limited feedback to increase the output dc power without requiring the knowledge of CSI.

V. CONCLUSIONS

We design, prototype, and experimentally validate a closed-loop WPT system with adaptive waveform and beamforming using limited feedback to increase the output dc power. Spatial and frequency domains are jointly exploited by adaptive multi-sine waveform and multi-antenna beamforming at the transmitter in WPT system to adapt the wireless multipath fading channel and increase the output dc power.

A closed-loop architecture for WPT based on a codebook design and a low complexity over-the-air limited feedback using an IEEE 802.15.4 RF interface is proposed. With the designed codebook and limited feedback, the channel estimation and accurate CSI can be avoided and more importantly the multi-sine waveform and multi-antenna beamforming at the transmitter can be optimized to adapt to the multipath fading channel in real time.

The proposed closed-loop WPT with adaptive waveform and beamforming using limited feedback is prototyped by a

Software Defined Radio equipment and measured in a real indoor environment. A closed-loop WPT system based on cable-feedback and an open-loop WPT system are also measured as comparison benchmarks. The measurement results show that using closed-loop adaptive multi-sine waveform and multi-antenna beamforming can effectively increase the output dc power. Compared with the conventional 1-tone 1-antenna WPT system, the proposed closed-loop WPT system with adaptive waveform and beamforming can increase the output dc power by up to 14.7 dB. In addition, compared with the cable-feedback based closed-loop WPT system, the proposed closed-loop WPT system using limited feedback can achieve similar performance while it is more practical and beneficial since it does not require any computationally complex and energy consuming channel estimation implementation at the receiver and does not rely on knowing the CSI accurately at the transmitter.

REFERENCES

- [1] Z. Popovic, "Cut the cord: Low-power far-field wireless powering," *IEEE Microwave Magazine*, vol. 14, no. 2, pp. 55–62, 2013.
- [2] C. Song, P. Lu, and S. Shen, "Highly efficient omnidirectional integrated multi-band wireless energy harvesters for compact sensor nodes of internet-of-things," *IEEE Trans. Ind. Electron.*, pp. 1–1, 2020.
- [3] S. Shen, C. Y. Chiu, and R. D. Murch, "A dual-port triple-band L-probe microstrip patch rectenna for ambient RF energy harvesting," *IEEE Antennas Wireless Propag. Lett.*, vol. 16, pp. 3071–3074, 2017.
- [4] V. Palazzi, J. Hester, J. Bitto, F. Alimenti, C. Kallialakis, A. Collado, P. Mezzanotte, A. Georgiadis, L. Roselli, and M. M. Tentzeris, "A novel ultra-lightweight multiband rectenna on paper for RF energy harvesting in the next generation LTE bands," *IEEE Transactions on Microwave Theory and Techniques*, vol. 66, no. 1, pp. 366–379, 2018.
- [5] S. Shen, Y. Zhang, C. Chiu, and R. Murch, "A triple-band high-gain multibeam ambient RF energy harvesting system utilizing hybrid combining," *IEEE Trans. Ind. Electron.*, vol. 67, no. 11, pp. 9215–9226, 2020.
- [6] S. Shen, C. Y. Chiu, and R. D. Murch, "Multiport pixel rectenna for ambient RF energy harvesting," *IEEE Trans. Antennas Propag.*, vol. 66, no. 2, pp. 644–656, Feb. 2018.
- [7] Y. Hu, S. Sun, H. Xu, and H. Sun, "Grid-array rectenna with wide angle coverage for effectively harvesting RF energy of low power density," *IEEE Transactions on Microwave Theory and Techniques*, vol. 67, no. 1, pp. 402–413, 2019.
- [8] E. Vandelle *et al.*, "Harvesting ambient RF energy efficiently with optimal angular coverage," *IEEE Trans. Antennas Propag.*, vol. 67, no. 3, pp. 1862–1873, March 2019.
- [9] S. Shen, Y. Zhang, C.-Y. Chiu, and R. Murch, "An ambient RF energy harvesting system where the number of antenna ports is dependent on frequency," *IEEE Trans. Microw. Theory Tech.*, vol. 67, no. 9, pp. 3821–3832, Sep. 2019.
- [10] S. Shen, Y. Zhang, C.-Y. Chiu, and R. Murch, "Directional multiport ambient RF energy-harvesting system for the internet of things," *IEEE Internet of Things Journal*, vol. 8, no. 7, pp. 5850–5865, 2021.
- [11] W. Lin and R. W. Ziolkowski, "Electrically small huygens CP rectenna with a driven loop element maximizes its wireless power transfer efficiency," *IEEE Trans. Antennas Propag.*, pp. 1–1, 2019.
- [12] A. Okba, A. Takacs, and H. Aubert, "Compact rectennas for ultra-low-power wireless transmission applications," *IEEE Transactions on Microwave Theory and Techniques*, vol. 67, no. 5, pp. 1697–1707, 2019.
- [13] L. Li, X. Zhang, C. Song, W. Zhang, T. Jia, and Y. Huang, "Compact dual-band, wide-angle, polarization-angle-independent rectifying metasurface for ambient energy harvesting and wireless power transfer," *IEEE Transactions on Microwave Theory and Techniques*, pp. 1–1, 2020.
- [14] M. A. Aldhaeebi and T. S. Almoncef, "Highly efficient planar metasurface rectenna," *IEEE Access*, vol. 8, pp. 214 019–214 029, 2020.
- [15] T. S. Almoncef, F. Erkmen, M. A. Alotaibi, and O. M. Ramahi, "A new approach to microwave rectennas using tightly coupled antennas," *IEEE Trans. Antennas Propag.*, vol. 66, no. 4, pp. 1714–1724, 2018.
- [16] J. Antonio Estrada *et al.*, "RF-harvesting tightly coupled rectenna array tee-shirt with greater than octave bandwidth," *IEEE Transactions on Microwave Theory and Techniques*, vol. 68, no. 9, pp. 3908–3919, 2020.

- [17] M. Huang, Y. L. Lin, J. Ou, X. y. Zhang, Q. W. Lin, W. Che, and Q. Xue, "Single- and dual-band rf rectifiers with extended input power range using automatic impedance transforming," *IEEE Transactions on Microwave Theory and Techniques*, vol. 67, no. 5, pp. 1974–1984, 2019.
- [18] J. Kimionis, A. Collado, M. M. Tentzeris, and A. Georgiadis, "Octave and decade printed UWB rectifiers based on nonuniform transmission lines for energy harvesting," *IEEE Transactions on Microwave Theory and Techniques*, vol. 65, no. 11, pp. 4326–4334, 2017.
- [19] S. Fan, Z. Yuan, W. Gou, Y. Zhao, C. Song, Y. Huang, J. Zhou, and L. Geng, "A 2.45-GHz rectifier-booster regulator with impedance matching converters for wireless energy harvesting," *IEEE Transactions on Microwave Theory and Techniques*, vol. 67, no. 9, pp. 3833–3843, 2019.
- [20] S. N. Daskalakis, A. Georgiadis, G. Goussetis, and M. M. Tentzeris, "A rectifier circuit insensitive to the angle of incidence of incoming waves based on a wilkinson power combiner," *IEEE Transactions on Microwave Theory and Techniques*, vol. 67, no. 7, pp. 3210–3218, 2019.
- [21] F. Zhao, D. Insera, G. Gao, Y. Huang, J. Li, and G. Wen, "High-efficiency microwave rectifier with coupled transmission line for low-power energy harvesting and wireless power transmission," *IEEE Transactions on Microwave Theory and Techniques*, pp. 1–1, 2020.
- [22] S. A. Rotenberg, S. K. Podilchak, P. D. H. Re, C. Mateo-Segura, G. Goussetis, and J. Lee, "Efficient rectifier for wireless power transmission systems," *IEEE Transactions on Microwave Theory and Techniques*, vol. 68, no. 5, pp. 1921–1932, 2020.
- [23] Z. Zeng, S. Shen, X. Zhong, X. Li, C.-Y. Tsui, A. Bermak, R. Murch, and E. Sánchez-Sinencio, "Design of sub-gigahertz reconfigurable RF energy harvester from -22 to 4 dBm with 99.8% peak MPPT power efficiency," *IEEE J. Solid-State Circuits*, vol. 54, no. 9, pp. 2601–2613, Sep. 2019.
- [24] J. Bitto, R. Bahr, J. G. Hester, S. A. Nauroze, A. Georgiadis, and M. M. Tentzeris, "A novel solar and electromagnetic energy harvesting system with a 3-D printed package for energy efficient internet-of-things wireless sensors," *IEEE Transactions on Microwave Theory and Techniques*, vol. 65, no. 5, pp. 1831–1842, 2017.
- [25] Y. Zhang, S. Shen, C. Y. Chiu, and R. Murch, "Hybrid RF-solar energy harvesting systems utilizing transparent multiport micromeshed antennas," *IEEE Transactions on Microwave Theory and Techniques*, vol. 67, no. 11, pp. 4534–4546, 2019.
- [26] Y. Zeng, B. Clerckx, and R. Zhang, "Communications and signals design for wireless power transmission," *IEEE Trans. Commun.*, vol. 65, no. 5, pp. 2264–2290, May 2017.
- [27] B. Clerckx, K. Huang, L. R. Varshney, S. Ulukus, and M.-S. Alouini, "Wireless power transfer for future networks: Signal processing, machine learning, computing, and sensing," *ArXiv*, 2101.04810, 2021.
- [28] A. Boaventura, D. Belo, R. Fernandes, A. Collado, A. Georgiadis, and N. B. Carvalho, "Boosting the efficiency: Unconventional waveform design for efficient wireless power transfer," *IEEE Microwave Magazine*, vol. 16, no. 3, pp. 87–96, 2015.
- [29] A. J. S. Boaventura *et al.*, "Spatial power combining of multi-sine signals for wireless power transmission applications," *IEEE Trans. Microw. Theory Techn.*, vol. 62, no. 4, pp. 1022–1030, Apr. 2014.
- [30] F. Bolos, J. Blanco, A. Collado, and A. Georgiadis, "Rf energy harvesting from multi-tone and digitally modulated signals," *IEEE Transactions on Microwave Theory and Techniques*, vol. 64, no. 6, pp. 1918–1927, 2016.
- [31] A. J. S. Boaventura and N. B. Carvalho, "The design of a high-performance multisine RFID reader," *IEEE Transactions on Microwave Theory and Techniques*, vol. 65, no. 9, pp. 3389–3400, 2017.
- [32] Z. Liu, Z. Zhong, and Y. Guo, "In vivo high-efficiency wireless power transfer with multisine excitation," *IEEE Transactions on Microwave Theory and Techniques*, vol. 65, no. 9, pp. 3530–3540, 2017.
- [33] A. Collado and A. Georgiadis, "Optimal waveforms for efficient wireless power transmission," *IEEE Microw. Wireless Compon. Lett.*, vol. 24, no. 5, pp. 354–356, May 2014.
- [34] B. Clerckx, A. Costanzo, A. Georgiadis, and N. Borges Carvalho, "Toward 1G mobile power networks: RF, signal, and system designs to make smart objects autonomous," *IEEE Microw. Mag.*, vol. 19, no. 6, pp. 69–82, Sep. 2018.
- [35] S. Shen and B. Clerckx, "Beamforming optimization for MIMO wireless power transfer with nonlinear energy harvesting: RF combining versus DC combining," *IEEE Trans. Wireless Commun.*, vol. 20, no. 1, pp. 199–213, 2021.
- [36] D. Belo, D. C. Ribeiro, P. Pinho, and N. Borges Carvalho, "A selective, tracking, and power adaptive far-field wireless power transfer system," *IEEE Transactions on Microwave Theory and Techniques*, vol. 67, no. 9, pp. 3856–3866, 2019.
- [37] B. Yang, X. Chen, J. Chu, T. Mitani, and N. Shinohara, "A 5.8-GHz phased array system using power-variable phase-controlled magnetrons for wireless power transfer," *IEEE Transactions on Microwave Theory and Techniques*, vol. 68, no. 11, pp. 4951–4959, 2020.
- [38] D. Masotti, A. Costanzo, M. Del Prete, and V. Rizzoli, "Time-modulation of linear arrays for real-time reconfigurable wireless power transmission," *IEEE Transactions on Microwave Theory and Techniques*, vol. 64, no. 2, pp. 331–342, 2016.
- [39] A. Costanzo and D. Masotti, "Smart solutions in smart spaces: Getting the most from far-field wireless power transfer," *IEEE Microwave Magazine*, vol. 17, no. 5, pp. 30–45, 2016.
- [40] P. S. Yedavalli, T. Riihonen, X. Wang, and J. M. Rabaey, "Far-field RF wireless power transfer with blind adaptive beamforming for internet of things devices," *IEEE Access*, vol. 5, pp. 1743–1752, 2017.
- [41] K. W. Choi, L. Ginting, P. A. Rosyady, A. A. Aziz, and D. I. Kim, "Wireless-powered sensor networks: How to realize," *IEEE Trans. Wireless Commun.*, vol. 16, no. 1, pp. 221–234, Jan 2017.
- [42] S. Abeywickrama, T. Samarasinghe, C. K. Ho, and C. Yuen, "Wireless energy beamforming using received signal strength indicator feedback," *IEEE Trans. Signal Process.*, vol. 66, no. 1, pp. 224–235, Jan 2018.
- [43] H. Zhang, Y. Guo, S. Gao, and W. Wu, "Wireless power transfer antenna alignment using third harmonic," *IEEE Microwave and Wireless Components Letters*, vol. 28, no. 6, pp. 536–538, 2018.
- [44] H. Zhang, Y. Guo, S. Gao, Z. Zhong, and W. Wu, "Exploiting third harmonic of differential charge pump for wireless power transfer antenna alignment," *IEEE Microwave and Wireless Components Letters*, vol. 29, no. 1, pp. 71–73, 2019.
- [45] S. D. Joseph, Y. Huang, S. S. H. Hsu, A. Alieldin, and C. Song, "Second harmonic exploitation for high-efficiency wireless power transfer using duplexing rectenna," *IEEE Transactions on Microwave Theory and Techniques*, pp. 1–1, 2020.
- [46] B. Clerckx and E. Bayguzina, "Waveform design for wireless power transfer," *IEEE Trans. Signal Process.*, vol. 64, no. 23, pp. 6313–6328, Dec 2016.
- [47] Y. Huang and B. Clerckx, "Large-scale multi-antenna multisine wireless power transfer," *IEEE Trans. Signal Process.*, vol. 65, no. 21, pp. 5812–5827, Nov 2017.
- [48] B. Clerckx and E. Bayguzina, "Low-complexity adaptive multisine waveform design for wireless power transfer," *IEEE Antennas Wireless Propag. Lett.*, vol. 16, pp. 2207–2210, 2017.
- [49] Y. Huang and B. Clerckx, "Waveform design for wireless power transfer with limited feedback," *IEEE Trans. Wireless Commun.*, vol. 17, no. 1, pp. 415–429, Jan 2018.
- [50] S. Shen and B. Clerckx, "Joint waveform and beamforming optimization for MIMO wireless power transfer," *IEEE Trans. Commun.*, pp. 1–1, 2021.
- [51] J. Kim, B. Clerckx, and P. D. Mitcheson, "Signal and system design for wireless power transfer: Prototype, experiment and validation," *IEEE Trans. Wireless Commun.*, vol. 19, no. 11, pp. 7453–7469, 2020.
- [52] J. Kim and B. Clerckx, "Range expansion for wireless power transfer using joint beamforming and waveform architecture: An experimental study in indoor environment," *IEEE Wireless Communications Letters*, pp. 1–1, 2021.
- [53] S. Shen, J. Kim, C. Song, and B. Clerckx, "Wireless power transfer with distributed antennas: System design, prototype, and experiments," *IEEE Trans. Ind. Electron.*, pp. 1–1, 2020.